Cukurova Medical Journal
ÇUKUROVA ÜNİVERSİTESİ TIP FAKÜLTESİ

Cukurova Med J 2026;51(1):65-78
DOI: 10.17826/cumj.1783528

RESEARCH

Effect of Undaria pinnatifida extract on wound healing and pro-inflammatory and anti-inflammatory cytokine modulation

Undaria pinnatifida ekstraktının yara iyileşmesi ve pro-inflamatuvar ve anti-inflamatuvar sitokin modülasyonu üzerindeki etkisi

Kadriye Yağmur Oruç[1], Aykut Oruç[2], Gökhan Ağtürk[3], Hakkı Oktay Seymen[2], Hasan Ege[4]

[1]Istinye University, Istanbul, Türkiye
[2]Istanbul University-Cerrahpaşa, Istanbul, Türkiye
[3]Haliç University, Istanbul, Türkiye
[4]Istanbul Arel University, Istanbul, Türkiye

Abstract

Purpose: The aim of this study was to investigate the effects of *U. pinnatifida* extract on the pro-inflammatory and anti-inflammatory cytokine profile during wound healing at 24, 48, and 72 hours in a scratch wound healing assay performed using the CCD-1072Sk human skin fibroblast cell line.

Materials and Methods: CCD-1072Sk Fibroblast cell line was cultured, and *U. pinnatifida* was extracted. A viability test was performed, and 0.24 µl/ml and 0.5 µl/ml doses of *U. pinnatifida* were selected. Scratch Wound Healing Assay was performed. Samples were collected at 0, 24, 48, and 72 hours. Interleukin-1 beta (IL-1β), tumor necrosis factor-alpha (TNF-α), interleukin-10 (IL-10), transforming growth factor-beta 1 (TGF-β1), and brain-derived neurotrophic factor (BDNF) levels were determined by ELISA, and apoptosis was determined by Annexin-V-FITC/PI staining. Proliferation and cell migration were examined.

Results: In the viability test, 0.24 µl/ml (115.2±2.8) and 0.5 µl/ml (126.7±8.2) of *U. pinnatifida* were found to be significant at 72 hours compared to the control group (CTL) (100.0±4.1). The most intense and fastest wound closure was observed in cells treated with U-0.5 µL at 72 hours. BDNF and anti-inflammatory IL-10 increased compared to CTL at 72 hours in 0.5 µl/ml. TNF-α and IL-1β decreased in all time points compared to CTL.

Conclusion: *U. pinnatifida* extract, applied at low and high doses, can significantly support wound healing and play a role in precisely controlling the healing process.

Keywords: CCD-1072Sk, fibroblast, scratch wound assay, *Undaria pinnatifida*, wound healing

Öz

Amaç: Bu çalışmanın amacı CCD-1072Sk insan deri fibroblast hücre hattı kullanılarak oluşturulan çizik yara hattı testinde *U. pinnatifida* ekstresinin 24., 48., 72. saatlerdeki yara iyileşmesi sürecinde proinflamatuar ve anti-inflammatuar sitokin profiline olan etkilerini incelemektir.

Gereç ve Yöntem: CCD-1072Sk fibroblast hücre hattı kültüre alınmış ve *U. pinnatifida* özütü çıkarılmıştır. Canlılık testi yapılmış ve *U. pinnatifida*'nın 0,24 µl/ml ve 0,5 µl/ml dozları seçilmiştir. Çizik yara iyileşme analizi gerçekleştirilmiştir. Örnekler 0, 24, 48 ve 72. saatlerde toplandı. İnterlökin-1 beta (IL-1β), tümör nekroz faktörü-alfa (TNF-α), interlökin-10 (IL-10), dönüştürücü büyüme faktörü-beta 1 (TGF-β1) ve beyin kaynaklı nörotrofik faktör (BDNF) düzeyleri ELISA ile, apopitoz ise Annexin-V-FITC/PI boyama yöntemi ile belirlendi. Hücre çoğalması ve göçü incelendi.

Bulgular: Canlılık testinde, *U. pinnatifida*'nın 0,24 µl/ml (115,2±2,8) ve 0,5 µl/ml (126,7±8,2) düzeyleri 24, 48 ve 72. saatlerde kontrol (CTL) (100,0±4,1) grubuna göre anlamlı bulundu. En yoğun ve en hızlı yara kapanması, 72. saatte U-0,5 µL ile tedavi edilen hücrelerde gözlendi. BDNF ve anti-inflamatuvar IL-10, 72. saatte 0,5 µl/ml'de CTL'ye kıyasla arttı. TNF-α ve IL-1β, CTL'ye kıyasla tüm zaman noktalarında azaldı.

Sonuç: Düşük ve yüksek dozlarda uygulanan *U. pinnatifida* ekstresi, yara iyileşmesini önemli ölçüde destekleyebilir ve iyileşme sürecinin hassas kontrolünde rol oynayabilir.

Anahtar kelimeler: CCD-1072Sk, fibroblast, çizik yara modeli, *Undaria pinnatifida*, yara iyileşmesi

Address for Correspondence: Kadriye Yağmur Oruç, Istinye University Faculty of Medicine Department of Physiology, Istanbul, Türkiye E-mail: yagmur.oruc@istinye.edu.tr
Received: 14.09.2025 Accepted: 27.01.2026

INTRODUCTION

Skin, which constitutes approximately 16% of body weight, acts as a barrier against external stimuli and is the largest organ of the body[1]. Maintaining skin integrity is essential for maintaining overall health. Burns, trauma, or surgical wounds, in which this integrity is disrupted, can cause not only physiological but also emotional and psychological stress. Therefore, therapeutic interventions applied to the treatment of such wounds are extremely important[2,3]. Pathological conditions and physiological processes such as obesity[4], diabetes[5], and aging[6] can deviate from the classic healing process, leading to scar formation and/or chronic wounds. In this context, patients become more vulnerable to infection, further diminishing their quality of life[2,3].

The wound healing process involves hemostasis, inflammation, proliferation, and remodeling, including cell migration, proliferation, and matrix deposition[7]. The interaction between cells and the extracellular matrix determines the rate of wound healing. Fibroblasts synthesize extracellular matrix components, macrophages secrete molecules that facilitate inflammation and repair, endothelial cells promote angiogenesis, and keratinocytes trigger epidermal regeneration[8,9]. These interactions are coordinated by cytokines[10]. By maintaining the balance of pro-inflammatory cytokines such as TNF-α (Tumor Necrosis Factor-alpha) and Interleukin-1β (IL-1β), which increase in the inflammation phase of wound healing, and anti-inflammatory cytokines such as interleukin-10 (IL-10) and TGF-β1 (Transforming Growth Factor-beta 1), which become more active in the proliferation and remodeling phase, keloids, hypertrophic scars[11] or inadequate inflammatory responses are prevented[12].

TNF-α, produced by macrophages in the early inflammatory phase, enhances the immune response. However, its overproduction leads to chronic inflammation and tissue damage, inhibiting wound healing[13,14]. IL-1β modulates the inflammatory phase by binding to IL-1 receptors (IL-1R) on the target cell membrane and activating nuclear factor-kappa beta (NF-κB), mitogen-activated protein kinase (MAPK), and Janus kinase/signal transducers and activators of transcription (JAK/STAT) signaling pathways, thereby increasing proinflammatory cytokine/chemokine production[15].

Interleukin-10 (IL-10) regulates excessive immune responses[16]. IL-10 increases anti-inflammatory genes via JAK-STAT pathway activation, inhibits NF-κB pathways, and exerts a dual effect during the remodeling phase via MAPK pathway activation, accelerating healing by supporting fibroblast-macrophage activation[17]. TGF-β1 increases fibroblast activation and collagen production by inhibiting proinflammatory cytokines and supports tissue repair at all stages, especially proliferation and remodeling, through the SMAD and MAPK pathways[18]. Brain-derived neurotrophic factor (BDNF), another important anti-inflammatory molecule in wound healing, activates the MAPK and Phosphoinositide 3-Kinase/Protein kinase B (PI3K/Akt) pathways through the Tropomyosin receptor kinase B (TrkB) receptor, and increases fibroblast activation and collagen production[19].

The discovery of natural compounds that promote wound healing and regulate cytokine balance is of great importance. In this context, *Undaria pinnatifida (U. pinnatifida)* (Harvey Suringar, 1873) an edible brown algae, has emerged as a promising resource in wound healing studies20. U. pinnatifida accelerates wound healing processes due to its richness in biologically active compounds such as fucoidans and phlorotannins[21]. Fucoidans are sulfated polysaccharides with anti-inflammatory, antioxidant, and wound-healing properties[22]. Phlorotannins are phenolic compounds with antioxidant and antimicrobial properties[23].

The original contribution of this study is to evaluate the effects of *U. pinnatifida* on cytokine changes during wound healing in vitro. In this study, a wound scratch assay was performed in vitro using the CCD-1072Sk human skin fibroblast cell line to investigate the effects of low and high doses of *U. pinnatifida* extract on cytokines involved in wound healing and on apoptosis.

MATERIALS AND METHODS

Procedure

Since this study was conducted solely using cell culture models, ethical committee approval was not required and therefore was not obtained. The study was carried out in the Physiology Research Laboratory of Haliç University Faculty of Medicine. All experiments and analyses were performed by experienced researchers involved in the study.

Experiments were performed in accordance with our institution's standard laboratory operating protocols. Cell culture procedures were carried out under aseptic conditions and according to pre-validated protocols. All experiments were performed in independent replicates. The same experimental conditions and equipment were used for each replicate.

CCD-1072Sk (ATCC-CRL-2088); USA) human skin fibroblast cells were obtained at the 5th passage by culturing in a sterile laminar cabinet. Mycoplasma contamination control was performed routinely and all cultures were negative. Dulbecco's modified eagle medium (DMEM, Gibco, Thermo Fisher) supplemented with 10% fetal bovine serum (Fetal Bovine Serum, Gibco, Thermo Fisher) and 1% antibiotic (100 UI/ml) (Penicillin/Streptomycin, Gibco, Thermo Fisher) was used. Cells were removed from the liquid nitrogen tank at -196°C, thawed gently, and transferred to 25 cm^2 flasks. The cells were incubated at 37°C and 5% CO2 (CO2 Incubator, MCO-170AC-PE, PHC Corporation, Japan). Cells were confirmed to have reached 85-90% confluency using a PrimoVert-Inverted microscope (Carl Zeiss Microscopy).

Trypsinization was performed by incubating with trypsin-EDTA (Gibco, Thermo Fisher) for 4 minutes at 37°C and 5% CO2. Cells were transferred to sterile tubes and centrifuged at 1300 RPM (300 × g, rotor radius: 12 cm) for 10 minutes, and the supernatant was discarded. Medium was added to the pellet, and the cells were placed in 25 cm^2 flasks and incubated at 37°C and 5% CO2. This process ensured that healthy cells were ready for use in the experiment. Ethical approval is not applicable to this study.

Plant material and extraction of *Undaria pinnatifida*

Dried *U. pinnatifida* seaweed was obtained from a commercial supplier (Fishing Corporation Open Food Co., Ltd; Batch number: 190555; product code: 03201). For extraction, 10 grams of dried *U. pinnatifida* were weighed and transferred to a sterile glass beaker[24]. 100 mL of 70% (v/v) ethanol was added to the beaker to achieve a solid-to-solvent ratio of 1:10. This standardized ethanolic extraction method was selected based on previously published protocols for marine algal extracts used in cell culture studies[21,25], which are known to yield reproducible fucoidan- and phlorotannin-enriched extracts. The beaker was covered with aluminum foil to protect the solution from light, and parafilm was used to prevent solvent evaporation.

The mixture was stirred with a magnetic stirrer at room temperature for 24 h. After incubation, the extract was filtered to separate the liquid phase from the solid residue. The residue was subjected to two additional extraction cycles with fresh 70% ethanol under the same conditions. All collected filtrates were pooled and stored in a volumetric flask at +4 °C until further processing.

The collected residue was concentrated using a rotary evaporator under reduced pressure at 40-45°C to remove ethanol and obtain crude *U. pinnatifida* extract. The crude extract was stored at -20°C for 7 days before use in experiments. The stock solution was prepared in Dimethyl sulfoxide (DMSO), and the final DMSO concentration in cell treatments was kept below 0.1%. Before cell culture application, all extracts were sterilized by passing through a 0.22 µm membrane filter.

Viability assay

To evaluate cell viability in the CCD-1072Sk fibroblast cell line, a 3-[4,5-dimethylthiazol-2-yl]-2,5-diphenyl-tetrazolium bromide (MTT) assay was performed. Cells were seeded into 96-well plates, with each well containing 5×10^4 cells. U. pinnatifida extract was added to the cells at concentrations of 0.00 (control, CTL), 0.015, 0.03, 0.06, 0.12, 0.24, and 0.5 µL, and incubated for 24, 48, and 72 hours. After incubation, 0.1 mg/mL MTT solution was added to each well. The cells were incubated for 4 hours to form formazan crystals. DMSO was added at a 300:1 ratio to dissolve formazan crystals. All experiments were performed in three independent replicates (n = 3) and included an appropriate DMSO vehicle control.

The absorbance of the resulting solutions was measured at 540 nm (auxiliary wavelength used to enhance detection sensitivity), 570 nm (main absorbance peak of formazan, used for quantitative analysis), and 590 nm (reference/background wavelength for optical correction) wavelengths using a spectrophotometer (Multiskan GO, Thermo Fisher Scientific). Cell viability was calculated using the formula %= (Mean absorbance of the treatment)/(Mean absorbance of the control) x 10025. Concentrations of 0.24 and 0.5 µL were selected, and the CTL, U-0.24, and U-0.5 groups were created.

Scratch wound healing assay

A total of 5 x 104 cells were seeded in 24-well plates. Cell confluence was verified at 85-90% using an inverted microscope. To establish the scratch wound model, a single straight scratch was introduced in the center of each well with a sterile 200 µL pipette tip. The wound line was examined at 0, 24, 48, and 72 hours using an inverted microscope, and gap coverage and cell migration were documented with an integrated camera at 40x magnification. Images were acquired with a 200 µm bar scale and 600 dpi resolution.

Migration and wound line closure area were measured using ImageJ software v1.54 (National Institutes of Health, Bethesda, MD, USA)26. Experiments were conducted in three technical replicates, and analyses were performed in a blinded manner. The percentage of the remaining wound gap was calculated from the percentage of wound closure and the gap area using pixel analysis. The mean value from 5 fields per well was used for analysis.

Enzyme-linked ımmunosorbent assay (ELISA) analyses

BDNF ng/mL (Cat. No. E1302Hu, BT-LAB, Shanghai, China), IL-10 pg/mL (Cat. No. E0102Hu, BT-LAB, China), IL-1β pg/mL (Cat. No. E0143Hu, BT-LAB, China), TNF-α ng/L (Cat. No. E0082Hu, BT-LAB, China), and TGF-β1 pg/mL (Cat. No. E0134Hu, BT-LAB, China) levels were measured in the supernatant of samples collected at 24, 48, and 72 hours using ELISA kits. The cell suspension was diluted with phosphate-buffered saline (PBS), pH 7.2-7.4, and the cell concentration per well was adjusted to 1 million/ml. Each sample was pipetted into the wells in triplicate. ELISA analysis was performed according to the manufacturer's instructions.

The suitability of the kits for fibroblast supernatant has been confirmed based on manufacturer validation, as stated in the manufacturer's manual. Measurements were taken at 450 nm. The standard curve was generated separately for each parameter by plotting the mean OD values measured for each standard (y-axis) against the corresponding concentrations (x-axis) using computer-based software (SkanIt Software, Thermo Fisher Scientific). Data were normalized to total protein amount.

Apoptosis

Apoptosis staining was performed using the Annexin-V-FITC/PI Apoptosis Kit (Elabscience Bionovation Inc., Cat. No: E-CK-A211, Texas, USA). Annexin V binds to Ca2+-dependent phosphatidylserine with high affinity, while apoptosis detection is achieved with propidium iodide (PI)27. CCD-1072Sk cells were seeded at a density of 3 × 104 cells/well in 24-well plates, and 85–90% confluency was confirmed under an inverted microscope. Each group was pipetted in triplicate. Apoptosis is performed depending on the manufacturer's instructions.

For apoptosis assessment, S-scan selected five fields per well for each group. Approximately 300–450 cells were photographed at 40x magnification with a 50 µm scale bar using an inverted fluorescence microscope. Automated cell counting was performed using ImageJ, and manual verification was conducted. Apoptosis images represent five randomly selected fields from each group at 40x magnification28. Green fluorescent signal shows Annexin V-positive (+) apoptotic cells, red fluorescent signal shows PI-positive (+) dead/necrotic cells, and "Merged" panels show the overlaid images of both stainings and double positive (+/+) late apoptotic cells. Early apoptosis (Annexin V+/PI−), late apoptosis (Annexin V+/PI+), and necrosis (Annexin V−/PI+) rates were quantified and reported as percentages of the total number of counted cells.

Statistical analysis

Statistical analyses were done by GraphPad Prism (Version 10.2.0, GraphPad Software, United States of America). Normality is evaluated using the Shapiro-Wilk Test, and homogeneity of data was evaluated using the Levene Test. The data were determined to be normally distributed and homogeneous. For the scratch test, gap percentage analysis was performed using a two-way repeated-measures ANOVA, and the Geisser–Greenhouse correction was applied to address violations of sphericity. Group comparisons for ELISA and MTT tests, and for Remaining Wound Gap %, were made using one-way ANOVA followed by post hoc Bonferroni tests. Apoptosis staining and percentages were calculated separately for early apoptosis (Annexin V^+/PI^-), late apoptosis (Annexin V^+/PI^+), and necrosis (Annexin V^-/PI^+) was calculated by counting per area using channel separation, fixed thresholding, and particle analysis in

ImageJ; area means were combined at the well level (n=3 wells/group-time technical replicate) and One-way ANOVA, and the Bonferroni test was used for multiple comparisons. Results for ELISA and MTT tests (n=3 wells/group-time technical replicate) are presented as mean ± standard deviation (SD). Values for the remaining wound gap % and the apoptosis % cell count are presented as %. P values <0.05 were considered statistically significant. To assess how different the groups were from each other, F-statistics (F = Between-group variance / Within-group variance), Coefficient of Determination (R^2) for the variance ratio, and Mean Difference (MD) (mean of the tested group - mean of the compared group) values were added.

RESULTS

Cell morphology analysis

When the time series of the control group was examined, at 24 hours (Fig. 1A), intercellular spaces with thin, long structures were observed, and the cell cover was sparse. By 48 hours (Fig. 1B), cell density had increased, the spaces had partially diminished, and cell-cell contact was more pronounced. These findings indicate that active cell migration was continuing. As a result of cell migration and/or proliferation, by 72 hours (Fig. 1C), the culture area was largely covered by cells, the spaces had significantly decreased, and the surface was more homogeneous, but not completely covered (Fig. 1).

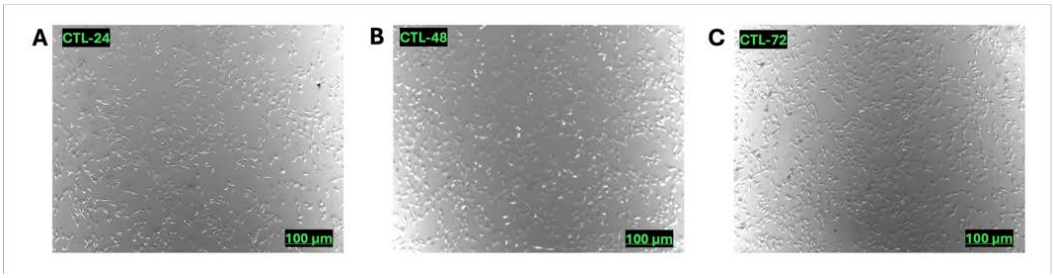


Figure 1. Cell morphology in the control (CTL) group. The CCD-1072D-Sk fibroblast cell line was examined at 24 (A), 48 (B), and 72 (C) hours. In the control group, cells maintained their normal morphological characteristics and did not show any obvious signs of degeneration or death. *(n = 3 technical replicates)*. Scale bar: 100 µm.

Viability assay analysis

U. pinnatifida extract concentrations of 0.015, 0.03, 0.06, 0.12, 0.24, 0.5 µL were analyzed in CCD-1072Sk fibroblast cell line by MTT assay at 24, 48, 72 hours time points (Fig. 2). A statistically significant difference was observed between the groups in MTT assessment at 24 hours ($F(6, 14)= 27.67$, $P<0.001$, $R^2= 0.9222$) (Fig. 2A). Significance was observed in the 0.5 group compared to CTL (MD =-14.55, $p<0.001$). A significant difference was observed in MTT assessment at 48 hours ($F(6,14)= 41.66$, $P<0.001$, $R^2= 0.9470$) (Fig. 2B). Compared to CTL, significant differences were observed in the 0.03 group (MD =8.920, $p=0.04$), 0.24 group (MD =-12.10, $p=0.004$), 0.5 group (MD =-21.87, $p<0.001$). A statistically significant difference was observed between the groups in the MTT assessment at the 72nd hour ($F(6, 14)=26.63$, $p<0.001$, $R^2=0.9195$) (Fig. 2C). Compared to CTL, significant differences were observed in the 0.24 group (MD =-15.24, $p=0.03$), 0.5 group (MD =-26.68, $p<0.001$). Values are given as mean ± standard deviation (SD) obtained from three independent experiments (Table 1). According to these results, U. pinnatifida doses for the experiments were determined as 0.24 and 0.5 µL.

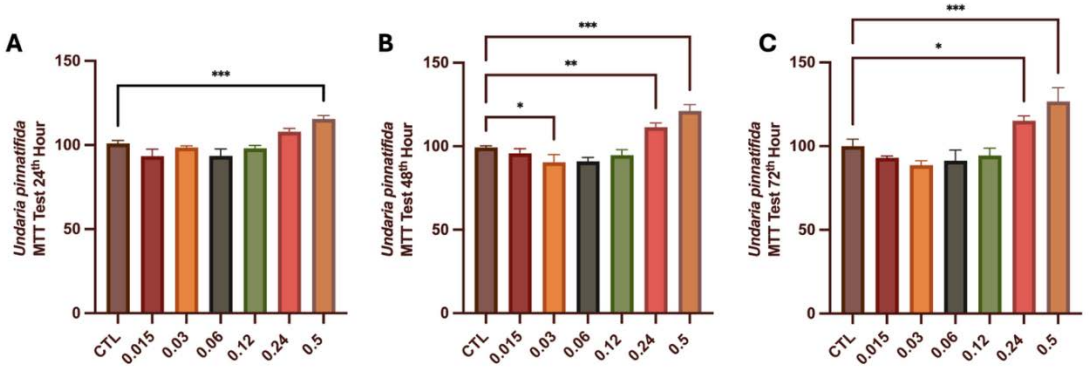


Figure 2. Effects of 0.015, 0.03, 0.06, 0.12, 0.24, 0.5 µL concentrations of U. pinnatifida extract on cell viability at 24, 48, and 72 hours. Cell viability was evaluated in the CCD-1072Sk fibroblast cell line by MTT assay. (A) 24-hour treatment results; (B) 48-hour treatment results; (C) 72-hour treatment results. CTL: Control group. Statistical analysis was performed by one-way ANOVA and the Bonferroni post-hoc test. Values are given as the mean ± standard deviation (SD) obtained from three independent experiments (n = 3 technical replicates). $p<0.05$ was considered significant. $p<0.05$*, $p<0.01$**, $p<0.001$***.

Table 1. Effect of 0.015, 0.03, 0.06, 0.12, 0.24, 0.5 µL concentrations of U. pinnatifida extract on cell viability at 24, 48 and 72 hours..

Undaria pinnatifida dosages	CTL	0.015	0.03	0.06	0.12	0.24	0.5
24 th hour	101.0±1.7	93.4±4.2	98.6±1.1	93.5±4.1	98.1±1.7	107.9±2.1	115.6±1.9
48 th hour	99.3±0.93	95.8±2.8	90.4±4.6	90.9±2.4	94.7±3.3	111.4±2.5	121.2±3.6
72 th hour	100.0±4.1	93.1±1.1	88.6±2.6	91.4±6.3	94.4±4.4	115.2±2.8	126.7±8.2

Cell viability was evaluated in the CCD-1072Sk fibroblast cell line by MTT assay. CTL: Control group. Statistical analysis was performed by one-way ANOVA and Bonferroni post-hoc test. Values are given as mean ± standard deviation (SD) obtained from three independent experiments ***(n = 3 technical replicates)***. $p<0.05$ was considered significant. ***p<0.05*, p<0.01**, p<0.001******

Scratch wound healing assay analysis

The effects of *U. pinnatifida* on wound healing were evaluated in CD-1072Sk cells. Progressive wound closure was observed in the control group at 24, 48, and 72 hours, with wound healing continuing at 72 hours. In the U-0.24 group, the remaining wound gap % remained stable compared to CTL at 24 and 48 hours, but greater closure was observed compared to CTL at 72 hours. In the U-05 group, healing, cellular migration, and proliferation were accelerated compared to the U-24 group at 48 hours. When evaluated by time point between groups, the most intense and fastest wound closure was observed in cells treated with U-0.5 µL at 72 hours (Fig. 3).

Remaining wound gap %

Statistical significance was found in the intergroup comparisons regarding the percentage of remaining wound gap after the addition of *U. pinnatifida* extract concentrations to the wound scratch test ($F(11, 24)=304.0$, $p<0.001$, $R^2 = 0.9929$). Compared to the CTL-0 group, significant statistical differences were observed in the CTL-24 (MD = 48.68, $p<0.001$), CTL-48 (MD = 66.4, $p<0.001$), and CTL-72 (MD = 70.0, $p<0.001$) groups. Compared to the U-0.24-0 group, significant statistical differences were found in the U-0.24-24 (MD = 54.19, $p<0.001$), U-0.24-48 (MD = 67.25, $p<0.001$), and U-0.24-72 (MD = 76.38, $p<0.001$) groups. Compared to the U-0.5-0 group, significant statistical differences were found in the U-0.5-24 (MD = 58.14, $p<0.001$), U-0.5-48 (MD = 72.62, $p<0.001$), and U-0.5-72 (MD = 88.17, $p<0.001$) groups. A significant difference was observed in the U-0.5-72 group compared to CTL-72 (MD = 14.19, $p<0.001$) (Fig. 4). [Figure 4 here]

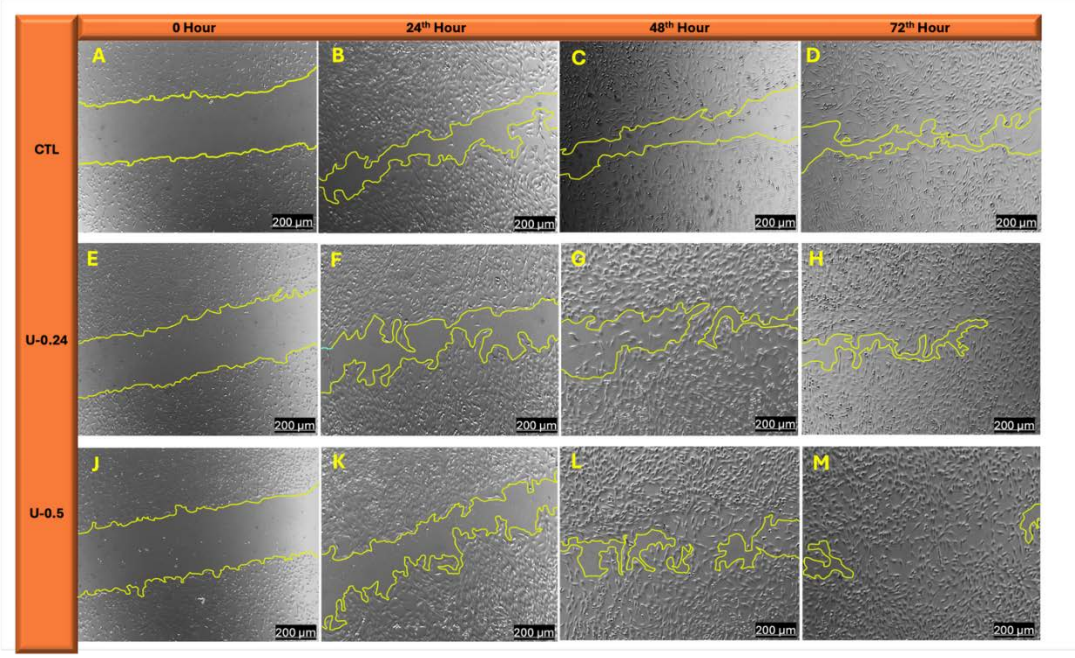


Figure 3. Effect of different concentrations of *U. pinnatifida* extract on cell migration.

Cell migration and gap closure were visualized at 0, 24, 48, and 72 hours using the scratch (wound healing) assay. Control group (A–D), U-0.24 group (E–H), and U-0.5 group (J–M). Yellow lines were automatically generated by ImageJ software to indicate wound edges. ***(n = 3 technical replicates).*** Images are raw images and were compiled into panels in PowerPoint; no digital processing was applied to cell morphology. Scale bar: 200 µm.

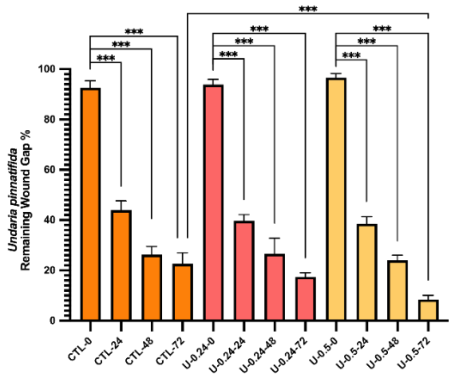


Figure 4. Quantification of the remaining wound gap percentage in CTL and Undaria pinnatifida-treated groups at 0, 24, 48, and 72 hours. Gap areas were quantified using ImageJ software (n = 3 technical replicates).

Data are expressed as mean ± SD. Statistical significance was assessed by one-way ANOVA followed by Bonferroni post hoc test $p<0.05$ accepted as significant . $p<0.05$*, $p<0.01$**, $p<0.001$***.

ELISA analysis

Statistical analysis were performed by one-way ANOVA and the Bonferroni post-hoc test. A significant statistical difference was observed between the groups in the IL-1β pg/mL ELISA ($F(1.614, 3.227)=340$, $p<0.001$, $R^2=0.9942$) (Fig. 5). Compared to the CTL-24 group, significant differences were found in the U-0.24-24 group (MD =1222, p=0.007), U-0.5-24 (MD =1618, p=0.01), and U-0.5-72 group compared to the CTL-72 group (MD =1905, p=0.05) (Fig. 5A).

A significant statistical difference was observed between the groups in the TNF-α ng/L ELISA ($F(1.646, 3.293)=147.8$, $p<0.001$, $R^2=0.9867$). A significant difference was found in U-0.5-48 (MD = 220.3, p=0.03) compared to the CTL-48 group and in U-0.24-72 (MD = 150.2, p=0.02) and U-0.5-72 (MD = 191.1, p=0.03) compared to the CTL-72 group (Fig. 5B).

A significant statistical difference was observed between the groups in the ELISA evaluation of

BDNF ng/mL (F(1.686, 3.373)=1821, p<0.001, R^2=0.9989). Compared to CTL-24 group at U-0.5-24 (MD =-1.468, p=0.02), compared to CTL-48 at U-0.24-48 (MD =-1.206, p<0.001), at U-0.5-48 (MD =-1.9, p=0.004), compared to CTL-72 at U-0.24-72 (MD =-1.007, p=0.02), at U-0.5-72 (MD =-2.115, p<0.001), compared to U-0.24-24 at U-0.24-48 (MD =-0.336, p=0.04) and compared to U-0.5-24 A significant statistical difference was found in U-0.5-72 (MD =-1.338, p=0.03) (Fig. 5C). A significant statistical difference was observed between the groups in the ELISA evaluation of IL-10 pg/mL (F(1.429, 2.859)=744.8, p<0.001, R^2=0.9973). Significant differences were found in the U-0.24-24 group compared to the CTL-24 group (MD =-52.34, p=0.02), in U-0.5-48 compared to the CTL-48 (MD =-162.4, p<0.001), in U-0.24-72 compared to the CTL-72 (MD =-194.9, p=0.01), in the U-0.5-72 group (MD =-211.7, p=0.02), and in U-0.5-72 compared to the U-0.5-24 (MD =-94.86, p=0.05) (Fig. 5D). No statistically significant difference was observed between the groups in the TGF-β1 ELISA evaluation (Fig. 5E).

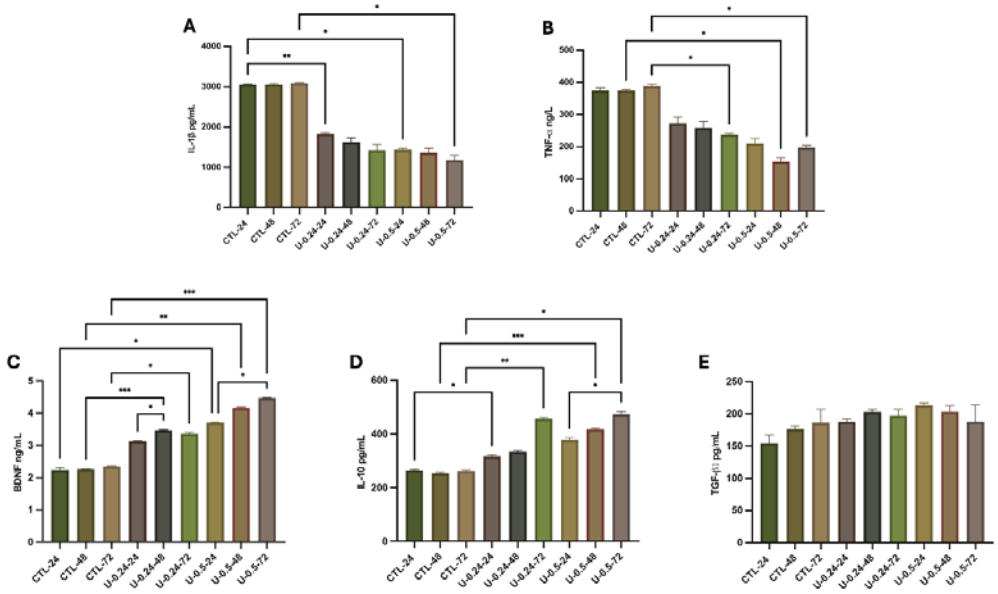


Figure 5. ELISA analyses of samples collected at 24, 48, and 72 hours with different concentrations of U. pinnatifida extract (0.24 µl, 0.5 µl). Proinflammatory cytokines were evaluated as (A) IL-1beta pg/mL; (B) TNF-alpha ng/L; anti-inflammatory cytokines as (C) BDNF ng/mL; (D) IL-10 pg/mL; (E) TGF-beta1 pg/mL.

CTL: Control group. Statistical analyses were performed by one-way ANOVA and Bonferroni post-hoc test. Analyses were pipetted in triplicate for each group (n = 3 technical replicates). Values are given as mean ± standard deviation (SD). p<0.05 was considered significant. p<0.05*, p<0.01**, p<0.001***.

Table 2. Effects of 0.24 µL and 0.5 µL concentrations of U. pinnatifida extract on the percentage of apoptotic cells at 24, 48, and 72 hours after scratch wound test in CCD-1072Sk cells.

	CTL-24	CTL-48	CTL-72	U-0.24-24	U-0.24-48	U-0.24-72	U-0.5-24	U-0.5-48	U-0.5-72
Apoptosis % Cell Count	1.40±0.1	1.63±0.1	1.33±0.2	1.23±0.6	2.36±0.4	6.53±0.5	5.30±0.3	4.13±0.2	3.43±0.5

Values are given as the mean ± standard deviation of the percentages obtained from three independent experiments (n = 3 technical replicates). CTL: control group.

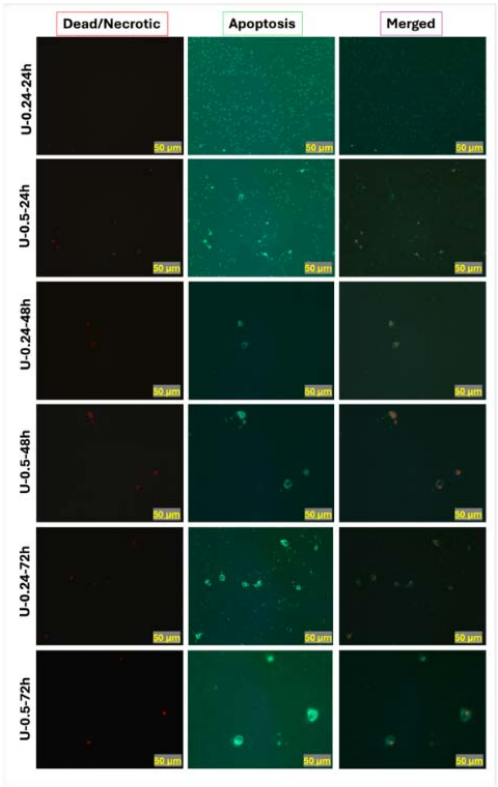


Figure 6. Results of Annexin V-FITC/PI double staining of 0.24 µL and 0.5 µL of *U. pinnatifida* extract in CCD-1072Sk fibroblast cell line. Cells were visualized by fluorescence microscope at 24, 48 and 72 hours.

Green fluorescent signal shows Annexin V-positive (+) apoptotic cells, red fluorescent signal shows PI-positive (+) dead/necrotic cells, and "Merged" panels show the overlaid images of both stainings and double positive (+/+) late apoptotic cells (n = 3 technical replicates). Images are raw and were only edited as panels in PowerPoint; no digital processing was applied to cell morphology. Images were taken under a fluorescence microscope at 20x objective magnification, scale bar: 50 µm.

Apoptosis analysis

In the U-0.24 group, Annexin V-positive (+) cells were observed at 24 hours, indicating early apoptosis. At 48 and 72 hours, a decrease in the number of PI-positive (+) cells, indicating necrotic/dead cells, was observed, but an increase in the number of cells was observed in merged photographs, indicating the double-positive (+/+) late apoptosis stage. In the U-0.5 group, early apoptosis was observed in Annexin V (+) cells at 24 hours, and late apoptosis was observed in cells that expressed high amounts of Annexin V/PI double-positive (+/+) signals at 48 and 72 hours (Fig. 6).

Apoptotic cell percentage was calculated as the ratio of Annexin V positive (early+late) cells in the total cell population. Statistically significant differences were observed in the evaluation of apoptotic cell percentage ($F(8, 18) = 89.22$, $P < 0.001$, $R^2 = 0.9754$). Significant statistical differences were detected in the U-0.5-24 group compared to CTL-24 (MD = -3.900, $p<0.001$), in U-0.5-48 compared to CTL-48 (MD = -2.500, $p<0.001$), in U-0.24-72 compared to CTL-72 (MD = -5.200, $p<0.001$), in U-0.5-72 (MD = -2.100, $p<0.001$), in U-0.5-24 compared to U-0.24-24 (MD = -4.067, $p<0.001$), in U-0.5-48 compared to U-0.24-48 (MD = -1.767, $p<0.001$), U-0.5-72 compared to U-0.24-72 (MD = 3.100, $p<0.001$) (Fig. 7, Table 2).

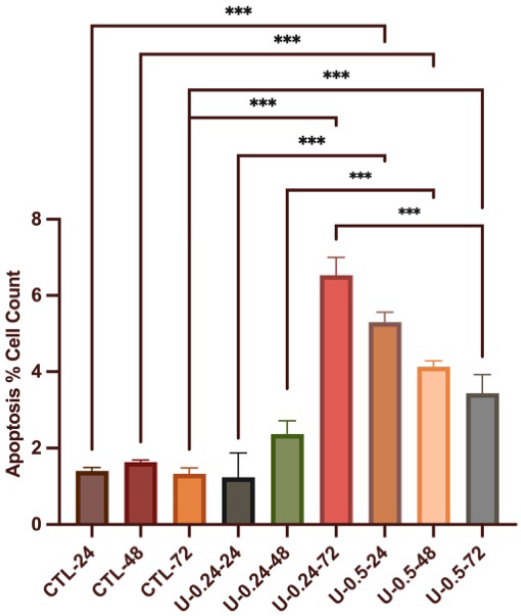


Figure 7. 0.24 µL and 0.5 µL of U. pinnatifida extract on the % apoptotic cell count at 24, 48 and 72 hours after scratch wound assay in CCD-1072Sk fibroblast cell line.

Apoptosis rate was calculated as the percentage of Annexin V-positive (early+late apoptosis) cells relative to the total cell number. Fluorescence microscope images after Annexin V-FITC/PI double staining were analyzed with ImageJ software (n = 3 technical replicates per group). CTL: control group. Statistical analysis was performed by one-way ANOVA and Bonferroni post-hoc test. Values are given as the mean ± SD of the percentages obtained from three independent experiments (n = 3 technical replicates). $p<0.05$ was considered significant. $p<0.05$*, $p<0.01$**, $p<0.001$***.

DISCUSSION

It is important to investigate natural compounds that promote wound healing and regulate cytokine balance. *U. pinnatifida* is a valuable resource for this purpose. This study examined the effects of low and high concentrations of *U. pinnatifida* extract on the wound healing phases and associated cytokines. The study evaluated the role of *U. pinnatifida* extract in accelerating the healing process by activating fibroblasts and exerting anti-inflammatory effects.

The molecular weight (kDa) of *U. pinnatifida* fucoidan is 168.5, and its chemical content includes 74.9 ± 3.4 sugars (%), 25.1 ± 1.4 sulfate (%). Sulfate content is a frequently studied property of fucoidan, as it is associated with the pharmacological activities of therapeutic agents[25]. Studies have reported that the sulfate content of U. pinnatifida varies between 7-38%[29,30]. These variations are reported to be normal since the molecular weight and sulfate content of polysaccharides depend on various factors such as the location and season of collection, the age of the seaweed, and the fucoidan extraction/purification method[25]. Fucoidans promote angiogenesis and accelerate wound healing through the Protein Kinase B/Nuclear factor erythroid 2–related factor 2/Hypoxia-inducible factor 1-alpha (AKT/Nrf2/HIF-1α) signaling pathway[31]. Low molecular weight fucoidan contained in *U. pinnatifida* has been shown to accelerate wound healing by increasing angiogenesis and collagen distribution in granular tissue[32]. In our study, the acceleration of cell migration to the wound line, increased cell proliferation and consequently increased wound closure rate at 24, 48 and 72 hours compared to the CTL group with the application of 0.24 and especially 0.5 µl concentrations. The decrease in remaining wound gap % reflects an increase in wound closure, suggesting that concentrations of U. pinnatifida accelerate and improve wound closure. This result is likely related to the high sulfate and sugar content of *U. pinnatifida.*

Antioxidant compounds are classified as primary (chain-breaking antioxidants) and reactive oxygen clearance, those that bind hydrogen (H+) atoms to free radicals, and secondary antioxidants (preventive antioxidants) that provide H+ to the primary antioxidant and act by breaking down hydrogen peroxide (H2O2)[33]. While copper chelation is a secondary antioxidant property[34], hydroxyl radical and H2O2 scavenging are primary antioxidant properties[35,36]. *U. pinnatifida* has primary and secondary antioxidant properties such as copper chelation due to its high sulfate content, hydroxyl radical scavenging activity, and H2O2 scavenging due to its high molecular weight[25,37].

In a study investigating the effect of *U. pinnatifida* fucoidans on the RAW 264.7 macrophage cell line, an MTT assay was performed, and it was reported that the reduction capacity of MTT dye to formazan crystals by mitochondrial enzymes was not reduced; cell viability and metabolic activity increased at doses of 2.5 mM and 5 mM, thus fucoidans had no cytotoxic effects[25,38]. The fact that 0.24 µl and 0.5 µl U. pinnatifida extracts we used in our study did not cause toxic effects and increased viability in the MTT test at 24, 48, and 72 hours is consistent with the literature.

In a model of oxidative damage in human renal proximal tubular epithelial cells (HK-2), it was reported that the healing rate was faster with the application of *U. pinnatifida* polysaccharide than with the control[39]. The cell migration and wound gap closure percentage data we obtained suggested that the fastest wound healing observed at the 72nd hour with the 0.5 µl dose was due to proliferative and migratory effects that paralleled the fucoidan concentration.

Increased TGF-β1 during wound healing plays a positive role in wound repair by promoting fibroblast repopulation and angiogenesis[40]. It has been reported that the expression of TGF-β1[41], released from fibroblasts via secretory autophagy during wound healing, begins to increase in the proliferative phase and reaches a peak level in the remodeling phase[42]. The absence of fibroblast-derived TGF-β1 leads to insufficient vascularization and impairs the maturation of granulation tissue in the early healing process[7]. No statistical changes were seen in TGF-β1 secretion from CCD-1072Sk fibroblast cells treated with *U. pinnatifida.* In this context, this suggests that *U. pinnatifida* does not disrupt the physiological TGF-β1 dynamics of fibroblasts during wound healing. Maintaining stable TGF-β1 levels is considered biologically consistent with normal granulation tissue formation and vascular maturation.

Apoptosis is a cellular clearance mechanism that functions in a controlled and effective manner during phase transitions during wound healing[43]. It increases

particularly during the inflammatory phase for the removal of inflammatory cells and during the remodeling phase required for successful scar tissue formation[44]. Apoptosis in both the U-0.24 and U-0.5 groups exhibited a time-dependent pattern consistent with physiological wound healing dynamics. In our data apoptotic activity showed a biological phase-aligned pattern: higher at 24 h (inflammatory phase), lower at 48 h (proliferative phase), and increased again at 72 h (remodeling phase). This pattern is consistent with the known temporal dynamics of apoptosis in wound healing. These statistically confirmed within-group temporal changes suggest that *U. pinnatifida* contributes to a balanced apoptotic response across healing phases.

Non-immune cell types, such as intestinal epithelial cells, intestinal fibroblasts, and skin keratinocytes, produce the anti-inflammatory cytokine IL-10 in response to stimuli such as injury, tissue damage, infection, and UV radiation45, 46. The tissue repair-promoting effect of IL-10 is due to the classical anti-inflammatory effects of IL-1016. The significant increases in IL-10 observed at 48 and 72 hours suggested that application of 0.5 μL of fucoidan supports tissue repair by enhancing the IL-10-mediated anti-inflammatory response in the late phase of wound healing. This finding is also consistent with the limited number of studies reporting both anti-inflammatory and pro-repair roles of IL-10.

Non-neuronal cells such as fibroblasts, endothelial cells, osteoblasts, and monocytes express BDNF[47,48]. BDNF activates the TrkB/Akt signaling pathway and regulates the expression of the cyclin-dependent kinase substrate 1 gene (NUCKS1), thereby promoting osteoblast proliferation and migration and enhancing fracture healing[48]. BDNF has also been reported to increase dermal fibroblast migration[49]. The increase in BDNF levels in all groups compared to CTL groups suggests that the healing-accelerating effect of *U. pinnatifida* fucoidan by promoting fibroblastic proliferation and migration is occur during the remodeling phase. In particular, the increase in BDNF levels with increasing dose indicates a concentration-dependent potentiation of fucoidan's contribution.

TNF-α and IL-1β are proinflammatory cytokines that play a role in the regulation of inflammation and are also produced by fibroblasts[50-52]. It has been reported that TNF-α levels increase significantly in both systemic and acute wounds and decrease in parallel with healing[53]. Dysregulation of IL-1β and TNF-α cytokines prolongs the inflammatory phase of wound healing and delays healing[54]. TNF-mediated inflammation has been reported to prevent TGF-β1-mediated normal wound healing and the development of fibrosis55. The gradual decrease in TNF-α and IL-1β levels in the CCD-1072Sk fibroblast cell line following fucoidan administration, compared to CTLs, was dose-dependent, indicating that healing progressed in a controlled manner by suppressing the excessive proinflammatory response. Additionally, the lack of significant change in TGF-β1 levels and the decrease in TNF-α suggest that fucoidan-mediated maintenance of the inflammation-repair balance prevents fibrosis and scar tissue formation. This further supports the opposing regulatory relationship between TNF-α and TGF-β1 reported in the literature.

Further studies examining the roles of *U. pinnatifida* in wound healing at 1, 3, 6, 9, and 12 months in the chronic phase could provide additional contributions to this research. Genetic and molecular-level investigations should be conducted to determine which protein family *U. pinnatifida* directly influences in wound healing.

This study has several limitations. As an in vitro fibroblast model, the generalizability of the findings to in vivo wound healing dynamics is limited. Extract concentrations were reported in μL rather than standard mass-based units (e.g., μg/mL), which may limit comparability across studies. Cytokine assessment was limited to a five-marker ELISA panel, and broader inflammatory profiling may provide additional information about the immunomodulatory effects of *U. pinnatifida*. Protein- and gene-level analysis (Western blotting, PCR) was not performed. No specific signaling molecules that could provide mechanistic insights were investigated. While apoptotic activity was assessed, no positive or negative control groups were included. The fucoidan, phlorotannin, sulfate and sugar content of the *U. pinnatifida* extract was not determined. The study was designed as a biological screening and preliminary mechanistic investigation, rather than as a phytochemical characterization study. Despite these limitations, the findings provide original preliminary data regarding the potential positive role of *U. pinnatifida* extract in wound healing.

Our findings showed that 0.24 μl/ml and 0.5 μl/ml doses of *U. pinnatifida* increased cell viability, migration, and proliferation in a dose- and time-

dependent manner. By inducing greater fibroblast activation, wound healing was supported, particularly during the proinflammatory and remodeling phases. *U. pinnatifida* extract exhibited a time-dependent oscillatory pattern in apoptosis, demonstrating its role in creating a balanced and uniform environment during healing. *U. pinnatifida* fucoidan at 0.24 µl/ml and 0.5 µl/ml resulted in a gradual increase in anti-inflammatory cytokines BDNF and IL-10 in a dose- and time-dependent manner, thereby accelerating fibroblast migration and tissue repair. The decrease in proinflammatory TNF-α and IL-1β levels supports the fact that the inflammatory phase (24 hours) can be maintained without exceeding fucoidan-mediated physiological limits, thus increasing the rate of healing. In conclusion, it was observed that *Undaria pinnatifida* extract, applied at low and high doses, can significantly support wound healing and play a role in precisely controlling the healing process.

Author Contributions: Concept/Design : KYO, AO, GA.; Data acquisition: KYO, AO, GA; Data analysis and interpretation: KYO, AO, Drafting manuscript: KYO, AO, HE; Critical revision of manuscript: KYO, AO, GA; Final approval and accountability:KYO, AO, GA, HOS, HE; Technical or material support: AO, KYO, GA, HOS, HE; Supervision: KYO, AO; Securing funding (if available): n/a.
Ethical Approval: This study was conducted in vitro and therefore did not require ethical committee approval. The cell line used in the study was purchased from the American Type Culture Collection (ATCC).
Peer-review: Externally peer-reviewed.
Conflict of Interest: Authors declared no conflict of interest.
Financial Disclosure: Authors declared no financial support
Acknowledgement: The research was carried out with the valuable support of the Physiology Laboratories at Haliç University-Faculty of Medicine.
This study has not been presented as a congress or presentation anywhere before.

REFERENCES

1. Díaz-García D, Filipová A, Garza-Veloz I, Martinez-Fierro ML. A Beginner's introduction to skin stem cells and wound healing. Int J Mol Sci. 2021;22:11030.
2. Mamun AA, Shao C, Geng P, Wang S, Xiao J. Recent advances in molecular mechanisms of skin wound healing and its treatments. Front Immunol. 2024;15:1395479.
3. Rodrigues M, Kosaric N, Bonham CA, Gurtner GC. Wound healing: a cellular perspective. Physiol Rev. 2019;99:665-706.
4. Cotterell A, Griffin M, Downer MA, Parker JB, Wan D, Longaker MT. Understanding wound healing in obesity. World J Exp Med. 2024;14:86898.
5. Song Y, You Y, Xu X, Lu J, Huang X, Zhang J et al. Adipose-derived mesenchymal stem cell-derived exosomes biopotentiated extracellular matrix hydrogels accelerate diabetic wound healing and skin regeneration. Adv Sci (Weinh). 2023;10:e2304023.
6. Kremer M, Burkemper N. Aging skin and wound healing. Clin Geriatr Med. 2024;40:1-10.
7. Peña OA, Martin P. Cellular and molecular mechanisms of skin wound healing. Nat Rev Mol Cell Biol. 2024;25:599-616.
8. Cheng X, Zhou J. Editorial: Advances in wound repair and regeneration: novel materials, targets and applications. Front Chem. 2024;12:1487091.
9. Gurtner GC, Werner S, Barrandon Y, Longaker MT. Wound repair and regeneration. Nature. 2008;453:314-21.
10. Burian EA, Enevold C, Karlsmark T, Ågren MS. Cytokine stability in chronic wound fluid and its association to fibroblast proliferation. Wound Repair Regen. 2024;32:704-8.
11. Wang ZC, Zhao WY, Cao Y, Liu YQ, Sun Q, Shi P et al. The roles of inflammation in keloid and hypertrophic scars. Front Immunol. 2020;11:603187.
12. Prakash M, Mathikere Naganna C, Radhakrishnan V, Somayaji P, Sabu L. Therapeutic potential of silkworm sericin in wound healing applications. Wound Repair Regen. 2024;32:916-40.
13. Yusuf K. The role of TNF-alpha in the wound healing process: molecular and clinical perspectives-a systematic literature review. Jurnal RSMH Palembang. 2022;3:222-8.
14. Lopes FB, Sarandy MM, Novaes RD, Valacchi G, Gonçalves RV. OxInflammatory responses in the wound healing process: a systematic review. Antioxidants (Basel). 2024;13:823.
15. Zaidi MB, Khan F, Jameel F, Khan I, Musharraf SG, Salim A et al. Temporal and differential proteomic profile of molecular mediators associated with chronic and acute wound healing. Cell Biochem Funct. 2024;42:e3946.
16. Saraiva M, Vieira P, O'Garra A. Biology and therapeutic potential of interleukin-10. J Exp Med. 2020;217:e20190418.
17. Hovsepian E, Penas F, Siffo S, Mirkin GA, Goren NB. IL-10 inhibits the NF-ʁB and ERK/MAPK-mediated production of pro-inflammatory mediators by up-regulation of SOCS-3 in Trypanosoma cruzi-infected cardiomyocytes. PLoS One. 2013;8:e79445.
18. Wynn TA, Barron L. Macrophages: master regulators of inflammation and fibrosis. Semin Liver Dis. 2010;30:245-57.
19. Harvey T, Rios M. The role of BDNF and TrkB in the central control of energy and glucose balance: an update. Biomolecules. 2024;14:424.
20. Coniglio D, Bianco M, Ventura G, Calvano CD, Losito I, Cataldi TRI et al. Lipidomics of the edible brown alga wakame (Undaria pinnatifida) by liquid chromatography coupled to electrospray ionization and tandem mass spectrometry. Molecules. 2021;26:4480.
21. Ferreira CAM, Félix R, Félix C, Januário AP, Alves N, Novais SC et al. A Biorefinery approach to the biomass of the seaweed Undaria pinnatifida (Harvey

Suringar, 1873): obtaining phlorotannins-enriched extracts for wound healing. Biomolecules. 2021;11:461.
22. Zayed A, Avila-Peltroche J, El-Aasr M, Ulber R. Sulfated galactofucans: an outstanding class of fucoidans with promising bioactivities. Mar Drugs. 2022;20:412.
23. Moeini A, Pedram P, Makvandi P, Malinconico M, d'Ayala GG. Wound healing and antimicrobial effect of active secondary metabolites in chitosan-based wound dressings: A review. Carbohydr Polym. 2020;233:115839.
24. Park JS, Han JM, Park SW, Kim JW, Choi MS, Lee SM et al. Subcritical water extraction of water extraction of Undaria pinnatifida: comparative study of the chemical properties and biological activities across different parts. Mar Drugs. 2024;22:344.
25. Silva MMCL, Dos Santos Lisboa L, Paiva WS, Batista LANC, Luchiari AC, Rocha HAO et al. Comparison of in vitro and in vivo antioxidant activities of commercial fucoidans from Macrocystis pyrifera, Undaria pinnatifida, and Fucus vesiculosus. Int J Biol Macromol. 2022;216:757-67.
26. Martinotti S, Ranzato E. Scratch wound healing assay. Methods Mol Biol. 2020;2109:225-9.
27. Kari S, Subramanian K, Altomonte IA, Murugesan A, Yli-Harja O, Kandhavelu M. Programmed cell death detection methods: a systematic review and a categorical comparison. Apoptosis. 2022;27:482-508.
28. Moela P, Motadi LR. RBBP6: a potential biomarker of apoptosis induction in human cervical cancer cell lines. Onco Targets Ther. 2016;9:4721-35.
29. Yu Y, Zhang Y, Hu C, Zou X, Lin Y, Xia Y et al. Chemistry and immunostimulatory activity of a polysaccharide from Undaria pinnatifida. Food Chem Toxicol. 2019;128:119-28.
30. Vaamonde-García C, Flórez-Fernández N, Torres MD, Lamas-Vázquez MJ, Blanco FJ, Domínguez H et al. Study of fucoidans as natural biomolecules for therapeutical applications in osteoarthritis. Carbohydr Polym. 2021;258:117692.
31. Wen W, Yang L, Wang X, Zhang H, Wu F, Xu K et al. Fucoidan promotes angiogenesis and accelerates wound healing through AKT/Nrf2/HIF-1α signalling pathway. Int Wound J. 2023;20:3606-18.
32. Park JH, Choi SH, Park SJ, Lee YJ, Song PH, Cho CM et al. Promoting wound healing using low molecular weight fucoidan in a full-thickness dermal excision rat model. Mar Drugs. 2017;15:112.
33. Flieger J, Flieger W, Baj J, Maciejewski R. Antioxidants: classification, natural sources, activity/capacity measurements, and usefulness for the synthesis of nanoparticles. Materials (Basel). 2021;14:4135.
34. Boulebd H, Spiegel M. Computational assessment of the primary and secondary antioxidant potential of alkylresorcinols in physiological media. RSC Adv. 2023;13:29463-76.
35. Sowndhararajan K, Kang SC. Free radical scavenging activity from different extracts of leaves of Bauhinia vahlii Wight & Arn. Saudi J Biol Sci. 2013;20:319-25.
36. Gulcin İ. Antioxidants and antioxidant methods: an updated overview. Arch Toxicol. 2020;94:651-715.
37. Čmiková N, Galovičová L, Miškeje M, Borotová P, Kluz M, Kačániová M. Determination of antioxidant, antimicrobial activity, heavy metals and elements content of seaweed extracts. Plants (Basel). 2022;11:1493.
38. Yang L, Liu J, Xia X, Wong IN, Chung SK, Xu B et al. Sulfated heteropolysaccharides from Undaria pinnatifida: Structural characterization and transcript-metabolite profiling of immunostimulatory effects on RAW264.7 cells. Food Chem X. 2022;13:100251.
39. Chen XW, Zheng YY, Ouyang JM. Sulfated Undaria pinnatifida polysaccharide promotes endocytosis of nano-calcium oxalate dihydrate by repairing subcellular organelles in HK-2 cells. Antioxidants (Basel). 2023;12:1015.
40. O'Leary R, Rerek M, Wood EJ. Fucoidan modulates the effect of transforming growth factor (TGF)-beta1 on fibroblast proliferation and wound repopulation in in vitro models of dermal wound repair. Biol Pharm Bull. 2004;27:266-70.
41. Nüchel J, Ghatak S, Zuk AV, Illerhaus A, Mörgelin M, Schönborn K et al. TGFB1 is secreted through an unconventional pathway dependent on the autophagic machinery and cytoskeletal regulators. Autophagy. 2018;14:465-86.
42. Willenborg S, Schönborn K, Sawant M, Bornikoel A, Yamane T, Zeinert I et al. Fibroblast-derived TGFβ1 regulates skin repair and fibrosis. Wound Repair Regen. 2025;33:e70065.
43. Greenhalgh DG. The role of apoptosis in wound healing. Int J Biochem Cell Biol. 1998;30:1019-30.
44. Riwaldt S, Corydon TJ, Pantalone D, Sahana J, Wise P, Wehland M et al. Role of apoptosis in wound healing and apoptosis alterations in microgravity. Front Bioeng Biotechnol. 2021;9:679650.
45. Carlini V, Noonan DM, Abdalalem E, Goletti D, Sansone C, Calabrone L et al. The multifaceted nature of IL-10: regulation, role in immunological homeostasis and its relevance to cancer, COVID-19 and post-COVID conditions. Front Immunol. 2023;14:1161067.
46. Jarry A, Bossard C, Bou-Hanna C, Masson D, Espaze E, Denis MG et al. Mucosal IL-10 and TGF-beta play crucial roles in preventing LPS-driven, IFN-gamma-mediated epithelial damage in human colon explants. J Clin Invest. 2008;118:1132-42.
47. Dudás J, Bitsche M, Schartinger V, Falkeis C, Sprinzl GM, Riechelmann H. Fibroblasts produce brain-derived neurotrophic factor and induce mesenchymal transition of oral tumor cells. Oral Oncol. 2011;47:98-103.
48. Meng W, Meng X, Han C, Li Y, Qian X, Zhang Z. BDNF improves fracture healing through promoting

osteoblasts proliferation and migration via trkb/akt regulated NUCKS1 expression. Sci Rep. 2025;15:27107.
49. Palazzo E, Marconi A, Truzzi F, Dallaglio K, Petrachi T, Humbert P et al. Role of neurotrophins on dermal fibroblast survival and differentiation. J Cell Physiol. 2012;227:1017-25.
50. Ramachandran T, Mohanraj KG, Mary Martin T, K MS. Enhanced wound healing with β-chitosan-zinc oxide nanoparticles: insights from zebrafish Models. Cureus. 2024;16:e69861.
51. Grivennikov SI, Tumanov AV, Liepinsh DJ, Kruglov AA, Marakusha BI, Shakhov AN et al. Distinct and nonredundant in vivo functions of TNF produced by t cells and macrophages/neutrophils: protective and deleterious effects. Immunity. 2005;22:93-104.
52. Ren K, Torres R. Role of interleukin-1beta during pain and inflammation. Brain Res Rev. 2009;60:57-64.
53. Ashcroft GS, Jeong MJ, Ashworth JJ, Hardman M, Jin W, Moutsopoulos N et al. Tumor necrosis factor-alpha (TNF-α) is a therapeutic target for impaired cutaneous wound healing. Wound Repair Regen. 2012;20:38-49.
54. Eming SA, Martin P, Tomic-Canic M. Wound repair and regeneration: mechanisms, signaling, and translation. Sci Transl Med. 2014;6:265sr6.
55. Steele H, Cheng J, Willicut A, Dell G, Breckenridge J, Culberson E et al. TNF superfamily control of tissue remodeling and fibrosis. Front Immunol. 2023;14:1219907.